

# Magnetic excitations in the normal and superconducting states of $\text{Sr}_2\text{RuO}_4$

F. Servant,<sup>1</sup> B. Fak,<sup>2,3</sup> S. Raymond,<sup>2</sup> J. P. Brison,<sup>1</sup> P. Lejay,<sup>1</sup> and J. Flouquet<sup>2</sup>

<sup>1</sup>Centre de Recherches sur les Très Basses Températures, CNRS, Boîte Postale 166, 38042 Grenoble, France

<sup>2</sup>Commissariat à l'Energie Atomique, Département de Recherche Fondamentale sur la Matière Condensée, SPSMS/MDN, 38054 Grenoble, France

<sup>3</sup>ISIS Facility, Rutherford Appleton Laboratory, Chilton, Didcot, Oxon OX11 0QX, Great Britain

(Received 17 January 2002; published 24 April 2002)

Inelastic-neutron-scattering measurements have been performed on single crystals of the spin-triplet superconductor  $\text{Sr}_2\text{RuO}_4$ . Incommensurate spin fluctuations were observed in both the normal and superconducting phases with the same intensity below and above  $T_c$ . Measurements of the wave-vector dependence of the magnetic scattering along the  $c$  axis suggest an itinerant character of the Ru form factor and an isotropic susceptibility.

DOI: 10.1103/PhysRevB.65.184511

PACS number(s): 74.70.Pq, 78.70.Nx, 75.40.Gb

## I. INTRODUCTION

The discovery<sup>1</sup> of superconductivity in  $\text{Sr}_2\text{RuO}_4$  has led to intensive efforts to establish the precise nature of the superconducting state. Most known superconductors are characterized by a spin-singlet state where the electrons in a Cooper pair have opposite spins. This is the case for conventional superconductors with  $s$ -wave symmetry ( $l=0$ ) and some high- $T_c$  cuprates with  $d$ -wave symmetry ( $l=2$ ).  $\text{Sr}_2\text{RuO}_4$ , on the other hand, is characterized by spin-triplet state Cooper pairing with  $p$ -wave symmetry ( $l=1$ ). Spin-triplet pairing is also observed in superfluid  $^3\text{He}$  and in the heavy-fermion superconductor  $\text{UPt}_3$ , which, however, has a more complicated Fermi surface.

The precise nature of the pairing state in  $\text{Sr}_2\text{RuO}_4$  is still under debate. The temperature-independent  $^{17}\text{O}$  Knight shift was the persuasive evidence of its spin-triplet pairing.<sup>2</sup> In analogy to superfluid  $^3\text{He}$ , a nodeless  $p$ -wave superconductivity has been inferred,<sup>3</sup> suggesting that  $\text{Sr}_2\text{RuO}_4$  is either near a ferromagnetic instability or characterized by strong ferromagnetic spin fluctuations. However, recent experiments<sup>4-6</sup> on high purity  $\text{Sr}_2\text{RuO}_4$  single crystals show a low-temperature behavior consistent with the presence of nodes in the superconducting order parameter, very similar to the observation of  $d$ -wave superconductivity in the high- $T_c$  cuprates. Most recently, a possible  $f$ -wave symmetry of the order parameter has been investigated theoretically.<sup>7,8</sup>

The electronic structure of  $\text{Sr}_2\text{RuO}_4$  at the Fermi surface is determined by the  $4d$  orbitals of the Ru ions in the  $\text{Ru-O}_2$  planes. The four electrons of  $\text{Ru}^{4+}$  are in the three  $t_{2g}$  orbitals ( $d_{yz}$ ,  $d_{xz}$ , and  $d_{xy}$ ). The detailed shape of the metallic Fermi surface has been determined by quantum-oscillation measurements<sup>9</sup> and the deduced band structure has three metallic bands with two electronlike ( $\alpha$  and  $\gamma$ ) and one holelike  $\beta$  Fermi surfaces. The  $\gamma$  band is two dimensional whereas the  $\alpha$  and  $\beta$  sheets are quasi-one-dimensional and can be visualized as a set of parallel planes running in both the  $k_x$  and  $k_y$  directions responsible for a sizable nesting effect at  $\mathbf{k}_0 = (2\pi/3a, 2\pi/3a, 0)$ . The simple features of the Fermi surface could nevertheless lead to complex multiband phenomena, which may also be relevant to the superconductivity.<sup>10</sup>

The knowledge of the dynamical spin susceptibility  $\chi''(\mathbf{q}, \omega)$  and its evolution in the superconducting state is an essential microscopic information for the understanding of the nature of the pairing in  $\text{Sr}_2\text{RuO}_4$ . Sidis *et al.*<sup>11</sup> showed that the main contribution to  $\chi''(\mathbf{q}, \omega)$ , measured by inelastic neutron scattering (INS) on single crystals, corresponds to incommensurate (IC) fluctuations appearing for  $T < 200$  K with a characteristic wave vector of  $\mathbf{q}_0 = (0.3, 0.3, 0)$ , indexed in reciprocal lattice units (r.l.u.). This wave vector corresponds approximately to the nesting wave vector  $\mathbf{k}_0$  predicted by band-structure calculations.<sup>12</sup> These fluctuations are quasielastic and well described by a Lorentzian shape with a relaxation rate of the order of  $\Gamma = 11$  meV. The  $q$  dependence is Gaussian with an energy-independent width (full width at half maximum) of 0.12 (1) r.l.u., corresponding to a correlation length within the  $a$ - $b$  plane of  $\xi_{ab} = 10.4$  Å. Servant *et al.* confirmed this picture on single-crystal samples grown in Grenoble and clearly demonstrated the two-dimensional nature of the correlations ( $\xi_c = 0$ ).<sup>13</sup>

In this paper, we present inelastic-neutron-scattering measurements of the magnetic fluctuations in single crystalline  $\text{Sr}_2\text{RuO}_4$ . The details of the crystal growth, sample characterization, and the neutron-scattering experiments are given in Sec. II. Section III presents the evolution of the incommensurate spin fluctuations in the superconducting and normal states. The wave-vector dependence of the magnetic scattering, which gives information on the magnetic anisotropy and the form factor, is presented in Sec. IV. The discussion in Sec. V relates the neutron-scattering results to NMR measurements and to the superconducting properties of  $\text{Sr}_2\text{RuO}_4$ .

## II. EXPERIMENTAL DETAILS

Our INS measurements were performed on single crystals grown by the floating-zone method using a light furnace equipped with double-elliptical mirrors, starting from sintered rods of off-stoichiometric  $\text{Sr}_2\text{RuO}_4$ . A 7-cm long 4-mm diameter cylindrical single crystal of total weight of 4.1 g was grown along the (100) direction. Figure 1 shows the results of the ac-susceptibility measurements on the whole of this crystal. A diamagnetic signal appears below  $T_c^{\text{onset}}$

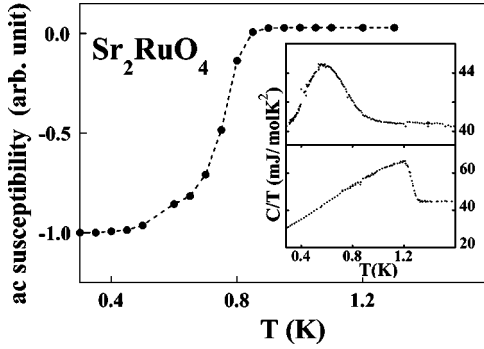


FIG. 1. Temperature dependence of the magnetic ac susceptibility of single-crystalline  $\text{Sr}_2\text{RuO}_4$ . The dashed line is a guide to the eyes. Inset: temperature dependence of the specific heat divided by temperature for two crystals with different superconducting transition temperatures.

$= 850$  mK and the width of the transition is  $\Delta T_c = 150$  mK. Specific-heat measurements using an adiabatic method were performed on a 64-mg piece cut from this crystal. The results, shown in the inset of Fig. 1, reveal a bump in the specific heat associated with the superconducting transition at  $T_c^{\text{onset}} = 850$  mK. This shows that the superconductivity of our sample has a bulk character. However, the specific jump  $\Delta C/C$  does not exceed 11% while for a small purer crystal ( $T_c = 1.29$  K), it reaches at least 52% and is quite comparable with published data (see inset of Fig. 1). X-ray-powder-diffraction measurements performed on small parts cut from the crystal used for the INS measurements do not reveal any traces of parasitic phases and the patterns were indexed with the body-centered tetragonal symmetry (space group  $I4/mmm$ ) and lattice parameters of  $a = 3.871$  and  $c = 12.745$  Å. The crystal was cut in three parts to allow for different orientations to be measured in the neutron-scattering experiments.

The INS measurements were performed on the IN22 triple-axis spectrometer installed on a thermal supermirror guide at the Institut Laue-Langevin, Grenoble, France, and operated by the CEA Grenoble. The (002) reflection of pyrolytic graphite (PG) crystals was used as vertically focusing monochromator and as horizontally focusing analyzer. Most measurements used a fixed final energy of  $E_f = 14.7$  meV and natural collimations. The corresponding energy resolution of the incoherent signal was 1.2 meV full width at half maximum (FWHM). A PG filter was placed between the sample and the analyzer in order to reduce higher-order contamination and the data were normalized by the incident beam monitor. A monitor count of 7000 corresponds approximately to 12 min counting time. The neutron-scattering intensity  $I(\mathbf{Q}, \omega)$  is proportional to the imaginary part of the dynamic magnetic susceptibility viz.

$$I(\mathbf{Q}, \omega) \propto \frac{1}{1 - \exp(-\hbar\omega/k_B T)} \chi''(\mathbf{Q}, \omega), \quad (1)$$

where  $k_B$  is Boltzmann's constant.

For the measurements of the correlations in the  $a$ - $b$  plane, the three crystals were mounted together and aligned with

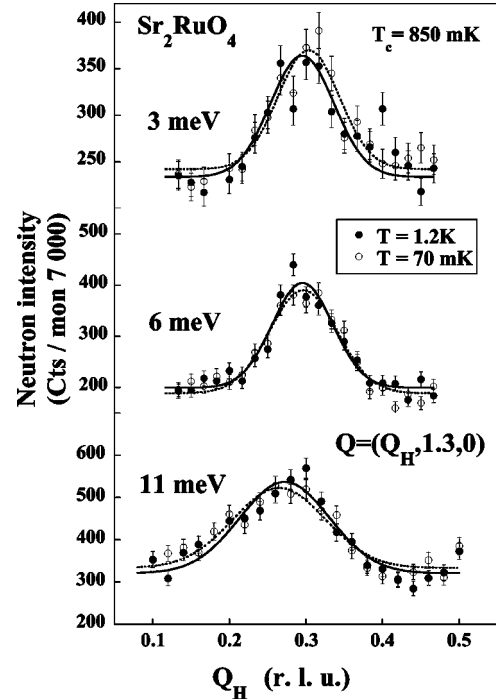


FIG. 2. Scans along the  $\mathbf{a}^*$  direction at  $\mathbf{Q} = (Q_H, 1.3, 0)$  for different energies as shown. The dashed and solid lines are fits to Gaussian functions at  $T = 70$  mK and 1.2 K, respectively.

the (100) and (010) axes in the horizontal-scattering plane and thermalized by a copper sheet attached to the mixing chamber of a  $^3\text{He}$ - $^4\text{He}$  dilution refrigerator. Measurements along the  $c$  axis were performed in a standard helium-flow cryostat with the (001) and (110) axes in the scattering plane of the spectrometer. The assembly of the three crystals has a mosaicity of  $0.6^\circ$  as measured on a rocking curve on the (200) Bragg reflection.

### III. INCOMMENSURATE SPIN FLUCTUATIONS IN THE SUPERCONDUCTING STATE

In order to investigate the spin fluctuations in the superconducting state, measurements were made at the base temperature of 70 mK and above  $T_c$ , at  $T = 1.2$  K. Figure 2 shows the result of scans along the  $\mathbf{a}^*$  direction at  $\mathbf{Q} = (Q_H, 1.3, 0)$  performed at different energy transfers of  $\omega = 3, 6,$  and  $11$  meV at these two temperatures (similar data obtained at 4 and 8 meV are not shown). At all energies and temperatures, the excitation spectrum is localized around the incommensurate wave vector  $\mathbf{Q}_0 = (0.3, 1.3, 0)$ , which is equivalent to the nesting vector  $\mathbf{k}_0 = (0.3, 0.3, 0)$  for two-dimensional fluctuations. The corresponding peaks have a Gaussian profile with an intrinsic width (FWHM) in  $Q_H$  of  $2\kappa_{ab} = 0.12$  (1) r.l.u., after correction for the instrumental  $Q$  resolution along the  $\mathbf{a}^*$  direction estimated from the (200) Bragg peak. The corresponding correlation length of the magnetic fluctuations is  $\xi_{ab} = a/(2\pi\kappa_{ab}) = 10.3$  (8) Å. Within the error bars, the peak intensities and widths are the same above and below  $T_c$ . Samples that do not exhibit superconductivity<sup>13</sup> have also the same correlation length  $\xi_{ab}$ .

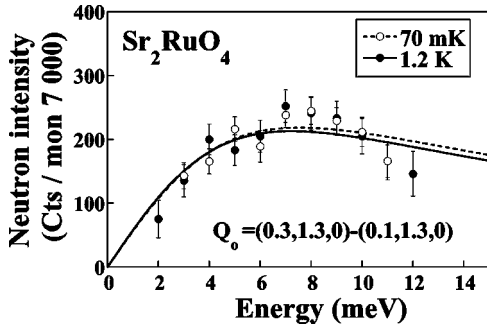


FIG. 3. Energy response of the magnetic signal at  $\mathbf{Q}_0 = (0.3, 1.3, 0)$  after subtraction of the background measured at  $\mathbf{Q}_1 = (0.1, 1.3, 0)$ . The dashed and solid lines are fits of a quasielastic Lorentzian [Eq. (2)] for the superconducting and normal phase, respectively.

For completeness, the spectral response at  $\mathbf{Q}_0 = (0.3, 1.3, 0)$  was measured as a function of neutron energy transfer below and above  $T_c$  (see Fig. 3). Given the strong phonon contribution, the spectrum is obtained by subtracting a background reference obtained at  $\mathbf{Q}_1 = (0.1, 1.3, 0)$  from the magnetic signal measured at  $\mathbf{Q}_0 = (0.3, 1.3, 0)$ . As already shown in previous studies, the imaginary part of the dynamical spin susceptibility corresponding to the measured signal is well described by a Lorentzian line shape

$$\chi''(\mathbf{Q}_0, \omega) = \chi'(\mathbf{Q}_0) \frac{\omega \Gamma}{\omega^2 + \Gamma^2}, \quad (2)$$

where  $\chi'$  is the static spin susceptibility and  $\Gamma$  the relaxation rate of the fluctuations. The solid line shown in Fig. 3 is a fit to Eqs. (1),(2) convoluted in one dimension with the resolution function. No significant changes between the data obtained at  $T_1 = 1.2$  K ( $> T_c$ ) and  $T_2 = 70$  mK ( $< T_c$ ) are observed: the result of the fit to Eqs. (1),(2) gives  $\Gamma_{T_1} = 7.6$  (9) and  $\Gamma_{T_2} = 7.2$  (9) meV. These values are smaller than that reported in Ref. 13, where the measurements were extended to higher energies, but are the same as that reported in Ref. 11. The difficulty to extract the relaxation rate  $\Gamma$  with precision is due to phonon contamination. Temperature sweeps at  $\mathbf{Q}_0$  and energies of 3 and 8 meV were performed in a search for anomalous behavior in the vicinity of the superconducting transition. No such effects were observed, as shown in Fig. 4.

As noted, our neutron-scattering data obtained on both sides of the superconducting transition in  $\text{Sr}_2\text{RuO}_4$  indicate no change in the dynamical spin susceptibility of the IC fluctuations, which dominate the magnetic excitation spectrum. There is no observation of a gap or of a transfer of spectral weight in the superconducting phase. The search for ferromagnetic fluctuations in both the normal and superconducting states was performed over a wide range of reciprocal space and energy (up to 34 meV), but no sizable magnetic signal was observed.

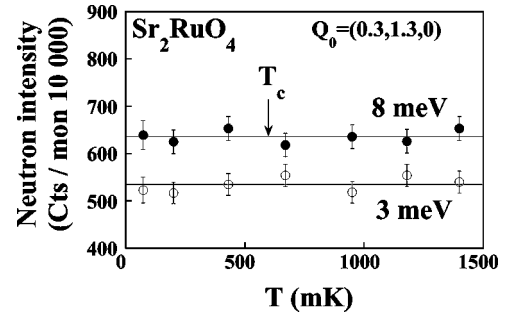


FIG. 4. Temperature dependence of the magnetic signal at  $\mathbf{Q}_0 = (0.3, 1.3, 0)$  for energy transfers of 3 and 8 meV.

#### IV. MAGNETIC ANISOTROPY AND FORM FACTOR

In Sec. III, we focused on the dynamical spin susceptibility *inside* a chosen Brillouin zone. This quantity reflects the correlations between spins and, for a Bravais lattice, it depends only on the reduced wave vector  $\mathbf{q} = \mathbf{Q} - \boldsymbol{\tau}$ , where  $\boldsymbol{\tau}$  is a reciprocal lattice vector and  $\mathbf{Q}$  is the total wave-vector transfer. In this section, we report detailed measurements of the total wave-vector transfer dependence of the neutron intensity over several Brillouin zones. This gives information on the anisotropy of the spin susceptibilities and the magnetic form factor of the Ru ion. The neutron intensity can be written as

$$I(\mathbf{Q}, \omega) \propto f^2(Q, \theta) [(1 + \sin^2 \theta) \chi''_{a,b}(\mathbf{q}, \omega) + \cos^2 \theta \chi''_c(\mathbf{q}, \omega)], \quad (3)$$

where  $f(Q, \theta) = f(\mathbf{Q})$  is the magnetic form factor and  $\theta$  the angle between  $\mathbf{Q}$  and the  $a$ - $b$  plane. The in-plane and out-of-plane susceptibilities are denoted  $\chi''_{a,b}$  and  $\chi''_c$ , respectively. To investigate the  $(Q, \theta)$  dependence of the magnetic scattering in  $\text{Sr}_2\text{RuO}_4$ , we measured the neutron intensity of the IC fluctuations along the  $c$  axis in several Brillouin zones.

Figure 5 shows constant  $\omega$  scans performed along the  $[1, 1, 0]$  direction around  $\mathbf{Q} = (0.3, 0.3, Q_L)$  for different fixed  $Q_L$  values at  $T = 1.5$  K and 6 meV energy transfer. The intensity clearly decreases with increasing  $Q$ , as expected from

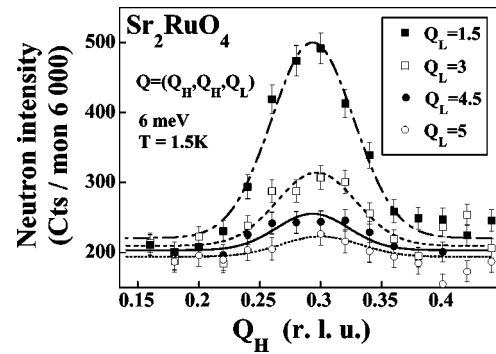


FIG. 5. Scans along the  $[110]$  direction around  $\mathbf{Q} = (0.3, 0.3, Q_L)$  for different fixed values of  $Q_L$  as shown at an energy transfer of 6 meV. The lines are fits to Gaussian functions. The data at  $Q_L = 3$  are shifted up by 25 counts and that at  $Q_L = 5$  are shifted down by 50 counts.

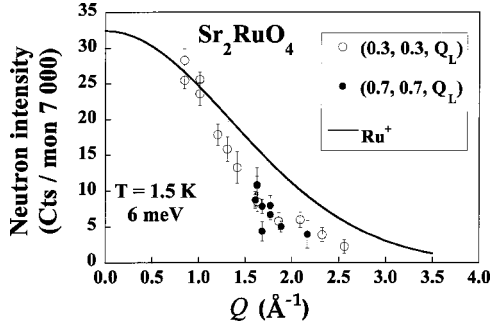


FIG. 6.  $Q$  dependence of the integrated magnetic intensity from scans along the [110] direction performed for different  $Q_L$  values on the two rods  $\mathbf{Q}_{r1}=(0.3,0.3,Q_L)$  and  $\mathbf{Q}_{r2}=(0.7,0.7,Q_L)$  at  $T=1.5$  K and an energy transfer of 6 meV. The solid line represents the  $\text{Ru}^+$  magnetic form factor.

the magnetic form factor. In order to get more insight on this behavior, such scans were performed for different  $Q_L$  values on the two rods  $\mathbf{Q}_{r1}=(0.3,0.3,Q_L)$  and  $\mathbf{Q}_{r2}=(0.7,0.7,Q_L)$  up to  $Q_L=5$  r.l.u. For each scan, the integrated intensity of the Gaussian line shape was extracted. This method is efficient in minimizing background effects and phonon contamination. Figure 6 shows the variation of these integrated intensities as a function of the magnitude of the wave vector. The decrease of the signal is faster than expected from a simple form factor of the  $\text{Ru}^+$  ion as shown in Fig. 6. This effect would probably be even more pronounced when compared with the  $4d$  orbitals in  $\text{Ru}^{4+}$ , which are likely to be more contracted than in  $\text{Ru}^+$ . It is worthwhile to note that the anisotropy of the magnetic form factor ( $\theta$  dependence) is negligible and not relevant for this study (the calculation is detailed in the Appendix).

The fact that the data obtained at  $\mathbf{Q}_{r1}$  and  $\mathbf{Q}_{r2}$  (full and empty circles in Fig. 6) fall on a same curve suggests an isotropic nature of the spin susceptibility. If the spin susceptibility were anisotropic, different intensities would be measured on the two rods, because they correspond to different values of  $\theta$  for a given value of  $Q$ . Since neutron-scattering probes only magnetic fluctuations perpendicular to the total wave-vector transfer  $\mathbf{Q}$ , the intensity observed near  $\theta=0$  is proportional to  $\chi''_{a,b} + \chi''_c$  and near  $\theta=90^\circ$  to  $2\chi''_{a,b}$  [see Eq. (3)]. As a consequence, for  $\chi''_{a,b} \neq \chi''_c$ , two different curves are expected as a function of  $Q$ . For example, in our case, the two wave vectors  $\mathbf{Q}=(0.3,0.3,3)$  and  $\mathbf{Q}=(0.7,0.7,0.5)$  have the same modulus,  $Q \approx 1.63 \text{ \AA}^{-1}$ , but different  $\theta$  angles,  $65^\circ$  and  $9^\circ$ , respectively. The susceptibilities probed are thus  $1.82\chi''_{a,b} + 0.18\chi''_c$  and  $1.02\chi''_{a,b} + 0.97\chi''_c$ , respectively. Within the error bars, the measured intensity is the same at these points, implying that  $\chi''_{a,b} \approx \chi''_c$ . Since large portions of reciprocal space were investigated in the present experiment, we checked carefully that resolution and absorption effects do not influence the measured integrated intensities. Resolution corrections are negligible since the IC fluctuations are broad in  $\mathbf{q}$  and  $\omega$ . Finally, we stress the importance of measuring at least two rods to address the anisotropy of the susceptibility. This allows a separation of the form factor and magnetic anisotropy contributions to the magnetic cross section when measuring at different values of  $Q_L$ . If the mag-

netic form factor was known with better precision, e.g., from polarized-neutron-scattering measurements, it would be simpler to determine the anisotropy of the susceptibility, as the intensity along only one rod would need to be measured.

In summary, our measurements of the two-dimensional correlations along the magnetic rods in  $\text{Sr}_2\text{RuO}_4$  suggest a substantially more delocalized magnetization density than expected from the  $\text{Ru}$  ion. In addition, the spin susceptibilities appear to be isotropic, in contrast to NMR measurements, as discussed in Sec. V A.

## V. DISCUSSION

### A. Excitations in the superconducting phase

The energy scale of the spin fluctuation relaxation rate  $\Gamma \approx 10$  meV, is two orders of magnitude larger than that of the superconducting transition  $k_B T_c \approx 0.1$  meV. It was pointed out by Monthoux<sup>14</sup> that the more relevant spin fluctuations for superconductivity have a ratio  $\Gamma/k_B T_c$  of the order of 10 for  $d$ -wave pairing and 100 for  $p$  wave. The latter ratio corresponds to the one observed here. Several groups<sup>15–17</sup> even predict resonance effects in the dynamical spin susceptibility that can be observed by INS in  $\text{Sr}_2\text{RuO}_4$ . These effects, well known for the high- $T_c$  compounds, give rise to enhanced scattering because of the coherence factor in the neutron-scattering cross section and they depend on the symmetry of the superconducting order parameter and the Fermi surface topology. For  $\text{Sr}_2\text{RuO}_4$ , the calculated resonance threshold<sup>15</sup> is two times smaller than the lowest energy accessible in the present experiment. This theory uses the gap energy  $\Delta_0=1$  meV obtained from a strong-coupling analysis of Andreev-reflection measurements.<sup>18</sup> In such a scenario, a resonance would be observed in INS data, most likely as a change of spectral weight between high and low energy. Such small changes are observed in the  $d$ -wave superconductor  $\text{La}_{1.86}\text{Sr}_{0.14}\text{CuO}_4$ ,<sup>19</sup> where the magnetic response is suppressed below 7 meV and enhanced above on cooling through  $T_c=35$  K. Our INS measurements were extended to lower energies by another group, but still no changes were observed in the dynamical spin susceptibility on cooling through  $T_c$ .<sup>20</sup>

The IC spin fluctuations correspond to transitions between the  $\alpha$  and  $\beta$  bands. In the extensively studied multiband superconductivity models,<sup>10,21</sup> the  $\alpha$  and  $\beta$  bands are the so-called passive bands while superconductivity is driven by the active  $\gamma$  band (the superconductivity of  $\text{Sr}_2\text{RuO}_4$  has the character of this main band as probed by  $H_{c2}$  and flux-line lattice measurements).<sup>22</sup> The relevance of spin fluctuations in the passive band for superconductivity is an open question. This depends among other factors on the coupling (hybridization) between the bands. The absence of evidence for two distinct superconducting phase transitions in high-quality single crystals, corresponding to the two types of bands, is a sign that superconductivity occurs as a global phenomena in this multiband system. The precise feedback mechanism between the IC fluctuations and the superconductivity is unknown in this context and is certainly not as simple as in a single-band picture. The effect of impurities could also help to distinguish between several theoretical

scenarios. The  $\alpha$  and  $\beta$  bands, which are believed to be responsible for the nodes in the order parameter, are more sensitive to the suppression of the superconductivity due to impurities than the  $\gamma$  band, which is compatible with nodeless superconductivity.<sup>21</sup> However, there is no change of the IC spin fluctuations across the superconducting transition, neither in our present measurements nor in those performed on crystals with higher  $T_c$ .<sup>20</sup> The  $\gamma$  band, on the other hand, give rise to  $q$ -independent fluctuations as evidenced by NMR.<sup>23</sup> These fluctuations have not been observed in INS studies, which can be understood if the spectral weight is spread out in  $q$  (in contrast to the relatively peaked IC fluctuations). An indirect comparison between NMR and INS results<sup>11,25</sup> suggests that these  $q$ -independent fluctuations are present in a wide temperature range (up to 500 K) and have a relaxation rate of about 50 meV.

### B. Anisotropy and form factor

Since the form factor represents the Fourier transform of the spatial extent of the wave function, the rapid drop off implies a more extended, and therefore itinerant nature of the Ru wave function. Including an orbital contribution  $L$  would make the character even more itinerant, since the shape of the theoretical ionic form factor would be even more localized (in direct space) with this extra contribution. Up to now, no precise determination of the magnetic form factor of  $\text{Sr}_2\text{RuO}_4$  is available.<sup>24</sup> In a previous INS study the form factor was estimated only in the basal plane with a limited accuracy.<sup>11</sup>

The  $p$ -wave state of  $\text{Sr}_2\text{RuO}_4$  is associated to an order parameter  $\mathbf{d}(\mathbf{k})$  describing the spin state and the wave-vector dependence of the superconducting gap. A state with  $\mathbf{d}$  parallel to the  $c$  axis and the spin in the basal plane is often assumed. This is supported by the NMR Knight shift ( $K$ ) measurements, which find no change of  $K$  on cooling through  $T_c$  for  $H$  in the basal plane.<sup>2</sup> Nevertheless, the question of the orientation of  $\mathbf{d}$  is not completely settled by these measurements due to the fact that no data could be obtained for  $H$  along the  $c$  axis ( $H_{c2}$  is too small in this direction). Several models deal with the possibility of having the pairing mechanism mediated by anisotropic IC fluctuations.<sup>15,26,27</sup> It is then expected that the orientation of the  $\mathbf{d}$  vector would reflect the anisotropy of the IC spin fluctuations. The NMR measurements by Ishida<sup>25</sup> suggest an anisotropic nature of the IC fluctuations with  $\chi_c''/\chi_a'' \approx 3$ . This is not confirmed by the present neutron-scattering study, where an isotropic behavior is found in a model-free analysis of the data. It is important to stress that the NMR results by Ishida<sup>25</sup> are based on the assumption that the hyperfine couplings are isotropic. Our results do not show links between the most commonly assumed spin-state of the superconducting order parameter and the IC spin fluctuations.

## VI. CONCLUSION

Our inelastic-neutron-scattering measurements performed on single crystals of  $\text{Sr}_2\text{RuO}_4$  reveal no changes in the incommensurate spin fluctuations on cooling through the su-

perconducting transition. By using the fact that these fluctuations are uncorrelated along the  $c$  axis (i.e., two dimensional), we also establish an isotropic nature of the incommensurate excitations together with a magnetic form factor that is more itinerant than the one expected for any known ruthenium ionic configuration. These new features may help to understand the relevance of the incommensurate spin fluctuations for the Cooper pairing, as investigated in several theoretical models. An unresolved issue is the multi-band nature of the superconductivity and its relation with the spin fluctuations observed in a passive band, which may nevertheless induce the pairing. Detailed form-factor measurements using a conventional polarized neutron method is highly desirable in order to confirm the itinerant character of the magnetization density in  $\text{Sr}_2\text{RuO}_4$ .

### ACKNOWLEDGMENTS

We would like to thank K. Ishida for useful discussions that motivated us to undertake the present measurements. We gratefully acknowledge J. Balay, A. Hadj-Azzem, and J.M. Martinod for technical assistance with sample preparation and characterization.

### APPENDIX: Ru FORM FACTOR

Here we briefly outline the calculation of the full  $\mathbf{Q}$  dependence of the magnetic form factor of Ru in  $\text{Sr}_2\text{RuO}_4$ . The  $Q$  dependence of the magnetic form factor of the  $\text{Ru}^+$  ion was used because that of  $\text{Ru}^{4+}$  has not been calculated theoretically.<sup>28</sup> Within the precision of our measurements, we could not distinguish between the Ru and  $\text{Ru}^+$  form factors, and  $\text{Ru}^{4+}$  is not expected to be very different from those. The magnetic form factor has two contributions coming from the two  $4d$  electrons present near the Fermi level. In a tetragonal environment, the  $4d$  levels involves one singlet  $d_{xy}$  and two doublets ( $d_{xz}, d_{yz}$ ) and ( $d_{x^2-y^2}, d_{z^2}$ ). In the ground state, the  $d_{xy}$  and ( $d_{xz}, d_{yz}$ ) orbitals are occupied. We assume that the orbital moment is quenched ( $L=0$ ) so that the form factor corresponds to pure spin contributions. The total form factor can then be written

$$F(\mathbf{Q}) = F(Q, \theta, \phi) = 2\langle j_0(Q) \rangle + [A_{xy}(\phi, \theta) + A_{xz, yz}(\phi, \theta)] \\ \times \langle j_2(Q) \rangle + [B_{xy}(\phi, \theta) + B_{xz, yz}(\phi, \theta)] \langle j_4(Q) \rangle,$$

where  $\langle j_n(Q) \rangle$  are spherical Bessel functions.<sup>28</sup> The angular dependence of the coefficients  $A$  and  $B$  for  $d$  electrons are given in Ref. 29. In our measurements, the azimuthal angle is  $\phi = 45^\circ$ . Numerical evaluation of these formula shows that the anisotropy ( $\theta$  dependence) of the form factor is very small. Consequently, the line shown in Fig. 6 is calculated for  $\theta = 0$ .

- <sup>1</sup>Y. Maeno, H. Hashimoto, K. Yoshida, S. Nishizaki, T. Fujita, J. G. Bednorz, and F. Lichtenberg, *Nature (London)* **372**, 532 (1994).
- <sup>2</sup>K. Ishida, H. Mukuda, Y. Kitaoka, K. Asayama, Z. Q. Mao, Y. Mori, and Y. Maeno, *Nature (London)* **396**, 658 (1998).
- <sup>3</sup>T. M. Rice and M. Sigrist, *J. Phys.: Condens. Matter* **7**, L643 (1995).
- <sup>4</sup>S. Nishizaki, Y. Maeno, and Z. Mao, *J. Phys. Soc. Jpn.* **69**, 572 (2000).
- <sup>5</sup>C. Lupien, W. A. MacFarlane, C. Proust, and L. Taillefer, *Phys. Rev. Lett.* **86**, 5986 (2001).
- <sup>6</sup>K. Ishida, H. Mukuda, Y. Kitaoka, Z. Q. Mao, Y. Mori, and Y. Maeno, *Phys. Rev. Lett.* **84**, 5387 (2000).
- <sup>7</sup>Y. Hasegawa, K. Machida, and Masa-aki Ozaki, *J. Phys. Soc. Jpn.* **69**, 336 (2000).
- <sup>8</sup>M. J. Graf and A. V. Balatsky, *Phys. Rev. B* **62**, 9697 (2000).
- <sup>9</sup>A. P. Mackenzie, S. R. Julian, A. J. Diver, G. J. McMullan, M. P. Ray, G. G. Lonzarich, Y. Maeno, S. Nishizaki, and T. Fujita, *Phys. Rev. Lett.* **76**, 3786 (1996).
- <sup>10</sup>D. F. Agterberg, T. M. Rice, and M. Sigrist, *Phys. Rev. Lett.* **78**, 3374 (1997).
- <sup>11</sup>Y. Sidis, M. Braden, P. Bourges, B. Hennion, S. Nishizaki, Y. Maeno, and Y. Mori, *Phys. Rev. Lett.* **83**, 3320 (1999).
- <sup>12</sup>I. I. Mazin and D. J. Singh, *Phys. Rev. Lett.* **82**, 4324 (1999).
- <sup>13</sup>F. Servant, S. Raymond, B. Fåk, P. Lejay, and J. Flouquet, *Solid State Commun.* **116**, 489 (2000).
- <sup>14</sup>P. Monthoux and G. G. Lonzarich, *Phys. Rev. B* **59**, 14 598 (1999).
- <sup>15</sup>D. K. Morr, P. F. Trautman, and M. J. Graf, *Phys. Rev. Lett.* **86**, 5978 (2001).
- <sup>16</sup>D. Fay and L. Tewordt, *Phys. Rev. B* **62**, 4036 (2000).
- <sup>17</sup>H. Y. Kee, *J. Phys.: Condens. Matter* **12**, 2279 (2000).
- <sup>18</sup>F. Laube, G. Goll, H. v. Löhneysen, M. Fogelström, and F. Lichtenberg, *Phys. Rev. Lett.* **84**, 1595 (2000).
- <sup>19</sup>T. E. Mason, A. Schröder, G. Aeppli, H. A. Mook, and S. M. Hayden, *Phys. Rev. Lett.* **77**, 1604 (1996).
- <sup>20</sup>M. Braden (private communication).
- <sup>21</sup>M. E. Zhitomirsky and T. M. Rice, *Phys. Rev. Lett.* **87**, 057001 (2001).
- <sup>22</sup>T. M. Riseman, P. G. Kealey, E. M. Forgan, A. P. Mackenzie, L. M. Galvin, A. W. Tyler, S. L. Lee, C. Ager, D. McK. Paul, C. M. Aegerter, R. Cubitt, Z. Q. Mao, T. Akima, and Y. Maeno, *Nature (London)* **396**, 242 (1998).
- <sup>23</sup>T. Imai, A. W. Hunt, K. R. Thurber, and F. C. Chou, *Phys. Rev. Lett.* **81**, 3006 (1998).
- <sup>24</sup>J. Duffy, S. Hayden, D. MckPaul, G. McIntyre and Y. Maeno, ILL Report No. 5-51-146, 2000 (unpublished).
- <sup>25</sup>K. Ishida, H. Mukuda, Y. Minami, Y. Kitaoka, Z. Q. Mao, H. Fukazawa, and Y. Maeno, *Phys. Rev. B* **64**, 100501 (2001).
- <sup>26</sup>T. Kuwabara and M. Ogata, *Phys. Rev. Lett.* **85**, 4586 (2000).
- <sup>27</sup>K. K. Ng and M. Sigrist, *J. Phys. Soc. Jpn.* **69**, 3764 (2000).
- <sup>28</sup>*International Tables of Crystallography*, edited by A. J. C. Wilson (Kluwer Academic, Dordrecht, 1995), Vol. C.
- <sup>29</sup>J. X. Boucherle, in *Electron and Magnetization Densities in Molecules and Crystals*, edited by P. Becker (Plenum, New York, 1980), p. 827.